The effect of changing the magnetic field strength on HiPIMS deposition rates

J W Bradley[1], A Mishra[1] and P J Kelly[2]

[1]*Department of Electrical Engineering and Electronics, University of Liverpool, Brownlow Hill, Liverpool L69 3GJ, UK*

[2]*Surface Engineering Group, Dalton Research Institute, John Dalton Building, Manchester Metropolitan University, Chester Street, Manchester, MI 5GD, UK*

Key words: Magnetron sputtering, HiPIMS, deposition rates, magnetic field strengths, back attraction, flux model

Correspondence: jw.bradley@liv.ac.uk

Abstract

The marked difference in behaviour between HiPIMS and conventional DC or pulsed-DC magnetron sputtering discharges with changing magnetic field strengths is demonstrated through measurements of deposition rate. To provide a comparison between techniques the same circular magnetron was operated in the three excitation modes at a fixed average power of 680 W and a pressure of 0.54 Pa in the non-reactive sputtering of titanium. The total magnetic field strength B at the cathode surface in the middle of the racetrack was varied from 195 to 380 G. DC and pulsed-DC discharges show the expected behaviour that deposition rates fall with decreasing B (here by ~ 25 to 40%), however the opposite trend is observed in HiPIMS with deposition rates rising by a factor of 2 over the same decrease in B.

These observations are understood from the stand point of the different composition and transport processes of the depositing metal flux between the techniques. In HiPIMS, this flux is largely ionic and slow post-ionized sputtered particles are subject to strong back attraction to the target by a retarding plasma potential structure ahead of them. The height of this potential barrier is known to increase with increasing B.

From a simple phenomenological model of the sputtered particle fluxes, using the measured deposition rates from the different techniques as inputs, the combined probabilities of ionization, α, and back attraction, β, of the metal species in HiPIMS has been calculated. There is a clear fall in αβ (from ~0.9 to ~0.7) with decreasing B-field strengths, we argue primarily due to a weakening of electrostatic ion back attraction, so leading to higher deposition rates. The results indicate that careful design of magnetron field strengths should be considered to optimise HiPIMS deposition rates.

1. Introduction

High power impulse magnetron sputtering (HiPIMS) is a relatively new ionized physical vapour deposition (IPVD) technique developed for the production of engineering-quality thin films [1]. It is characterized by high peak target power densities (several kW cm^{-2}) and high plasma densities (up to 10^{19} m^{-3}), providing in some cases metal ion-to-metal atom flux ratios at the substrate approaching unity, depending to the specific operating conditions [2]. To alleviate overheating of the target, HiPIMS discharges are operated with low duty cycles (<10%) and typically at low frequencies (<1 kHz). Although HiPIMS has provided new opportunities in pulsed sputtering, notably in the potential to control the direction and energy of the ionized metal flux, it is widely recognised that, at least in non-reactive sputtering, it suffers from significantly lower deposition rates than DC and pulsed DC magnetron sputtering [1, 2, 3].

Historically, much work has been done to understand and maximize deposition rates in conventional magnetron sputtering. For DC and mid-frequency sputtering deposition rates are observed practically to be directly proportional to the power applied to the target [4]. However, this is not the case for HiPIMS where the absolute deposition rate increases more slowly than at a linear rate with power [5]. Samuelsson et al [6] present a comparison between DC and HiPIMS deposition rates for a large variation of metal targets, concluding that HiPIMS deposition rates are between 2 and 5 times slower for the same power than DC. Interestingly, it has been observed that HiPIMS deposition rates increase with decreasing pulse length. This was demonstrated by Konstantinidis et al [7] who found that HiPIMS rates increase from 20 to 70% of DCMS values as the pulse length is decreased from 20 to 5 μs for the same average power. This phenomenon may be due to the fact that shorter pulse lengths do not allow a significant amount of gas rarefaction or self-sputtering to develop [8]. In general, deposition rates in the self-sputtering mode are found to be lower than when argon sputtering is dominating [9].

Since the deposition rate is an important, if not crucial, process parameter particularly in manufacturing, there has been keen interest in the HiPIMS research community to understand the cause of this deposition rate reduction [3] and so find methods to elevate it. Depending on the specific HiPIMS operating conditions there are number of factors that may lead to relatively low deposition rates in HiPIMS. These include:

1. A less than linear increase in sputtering yields with target voltage leading to lower sputter and deposition rates in HiPIMS since they operate at higher voltages than DC and mid-frequency pulsed magnetrons [3].
2. Tangential loss of post-ionized sputtered particles due to enhanced torodial ion transport in HiPIMS [10]. It is now thought that such azimuthal ion spin is produced by electric fields associated with rotating spoke structures at the target that accelerate metallic ions out of the discharge in the radial and axial directions [11].
3. The establishment of strong axial potential gradients in the HiPIMS plasma (pre-sheath region) that retard the transport of low energy post-ionized metal ions created close to the target to the substrate [12].
4. Significant gas rarefaction that can occur for longer HiPIMS pulses (> 50μs) causing a decrease in ions available for sputtering [7, 9].
5. High self-sputtering components in HiPIMS with associated self-sputter yields typically 10%–15% lower [3,8] than for Ar^+ sputtering and with projectile metal M^+ ions being lost so reducing the overall yield [2].

A number of suggestions have been proposed to improve the deposition rates in HIPIMS, including the use of an inductive coil placed in the discharge bulk, to bolster densities and metal post-ionisation probabilities [13] and the use of elevated target surface temperatures claimed to produce up to 1.9 times higher deposition rates [14 15]. Barker et al [15] showed that exciting the plasma with sequence of pulse packets separated by several hundred microseconds can increase HiPIMS deposition rates by up to 45%. Although the mechanisms for this are unknown the authors argue more time for gas refilling between packets and the prevention of self-sputtering may be important processes in this beneficial effect.

In an important contribution, Capek et al [16] showed that lowering the magnetic field in HiPIMS can have a profound effect on increasing the deposition rates. Using spacers of different widths behind the cathode to reduce the magnitude of the vacuum B-field at the target (and so increase the average discharge voltages at nominally simular powers) deposition rates of Nb were increased by a factor of 4.5. These results confirmed observation by Mishra et al [12] who found a six fold increase in the deposition rate of Ti for a by weakening the B-field by 33%.

Through comparisons of the amount of material lost from the cathode and the deposition rates between DC sputtering and HiPIMS (the latter with different B-field strengths), Capek et al [16] were able to quantity the relative faction of material lost through different processes in HiPIMS. To do this they developed a particle flux model in which the fraction of metal ions returning to the target, given by the product of the probabilities of ionisation and back attracting can be calculated. At high B-fields (and low average discharge voltages) a large proportion of metal ions return to the cathode with a small amount lost through (unknown) transport effects. However, at B-fields (higher discharge voltages) the return effect of ions to the target is greatly reduced, helping to increase deposition rates. In this case, a small yield effect due to significantly larger target voltages [3] starts to become more important, acting to reduce deposition rates.

In this study, we follow a similar approach to that in [16] to observer the effect of varying the magnetron magnetic field strength on HiPIMS deposition rates, but extend the investigation to also to DC and pulsed DC discharges. To illustrate the vast contrast in behaviour between these different modes of sputtering with changing B-field and to quantify the effects the same average power levels have been used throughout. Here we sputter a titanium target and vary the B-field strength with the aim to keep the same degree of un-balance in the field. Using a simple model, similar to that developed by Christie [17], assuming metal ions do not contribute to film formation in DC sputtering, and by comparing deposition rates from the different techniques, the compound probability of a metal ion being created in the plasma and returning to the target has been calculated for different field strengths in HiPIMS operation.

2. The experimental arrangement

A planar circular magnetron (V-TECH 150 supplied by GENCOA Ltd,) equipped with a 99.99% pure 150 mm diameter titanium target was used in this study. The magnetron was housed in a purpose built vacuum chamber (70 cm in length and 40 cm in diameter) which was pumped by a turbo-molecular pump backed by a rotary pump providing a base pressure of 2×10^{-6} Pa. The magnetic field strength of the magnetron was varied by moving the inner and outer magnetic poles using external Vernier screw gauges (a unique facility of this source). The deposition rate measurements were carried out 100 mm from the target at a position above the

racetrack (radial position r = 45 mm) using a Maxtek TM-400 multi film deposition rate monitor (equipped with 6 MHz quartz crystal oscillator and silver sensor). Although the arrival rate of the depositing flux varies during the pulse (for HiPIMS and mid-frequency sputtering), the slow response of the sensor allows only time-averaged values to be determined, in our case from the total thickness measured over a fixed deposition time of 120 s. The arrangement of the magnetron and deposition rate monitor is shown in figure 1. One important region of the discharge is the magnetic trap, defined by a region enclosed by magnetic field lines that intersect the target twice as shown in the figure. The magnetic field strengths and directions have been determined from bench measurements of the magnetic field taken in the axial (B_z) and radial directions (B_r) using a Hall probe. By withdrawing the magnets behind the target we were able to progressively lower the field strengths. The magnitude of total B-field $|B| = \sqrt{(B_z^2 + B_r^2)}$ along a line between the deposition rate monitor and the target is shown in figure 2. Here BF1 is the configuration with the highest fields, progressing down to the lowest in configuration BF4. As the magnets are withdrawn, $|B|$ drops by ~ 45 % at the target as can be seen in figure 2.

To create HiPIMS plasmas a SINEX 3.0 HiPIMS power supply (from Chemfilt Ion Sputtering) was used. The target was sputtered at frequencies of 75, 100 and 150 Hz, with a pulse-duration of 100 µs, in an argon gas environment (purity 99.99%) with time-averaged powers of 680 W (± 5%). The pressure was fixed at 0.54 Pa. For DC and pulsed-DC operation, the discharge was energized using a Pinnacle Plus$^+$ power supply from Advanced Energy Inc. also operating at 680 W with 0.54 Pa vessel pressure. In the latter mode, two frequencies were chosen namely, 100 and 350 kHz with 50% duty cycles in each case (i.e. pulse on-times of 5 and 1.43 µs, respectively). This power supply was operated in power regulation mode. Figure 3 shows the cathode voltage (V_d) and current (I_d) waveforms for the case of 100Hz HiPIMS at the four chosen magnetic field strengths BF1-BF4, to demonstrate the trends in each. The pulsed DC waveforms are not shown, as they are not our main interest here. V_d and I_d were measured at an intermediary aluminium test box placed between the power supplies and the magnetron source using a x100 voltage probe (P5100 Tektronix Ltd model) and a x20 current probe (Tektronix Ltd Model TCP 04) in conjunction with a x10 current probe (Tektronix Ltd Model TCP 202) for HiPIMS

measurements respectively. For HiPIMS measurements at each magnetic field configuration the discharge voltage was varied until the required average power P_{av} was achieved, (calculated on an oscilloscope in real time) using V_d (t) and I_d (t) via the equation;

$$P_{av} = \frac{1}{T}\int_0^T I_d\,(t)\;V_d\,(t)\,dt$$

where T is the pulse period frequency in each case. Clearly from figure 3 the peak in the discharge voltage V_d increases only marginally (by about ~ 5% at the peak) as the B-field at the target is reduced (by ~ 45%), however V_d values hold up significantly during the pulse as we go from BF1 to BF4. The average HiPIMS target voltages $\langle V_d \rangle$ increase from 246 to 511 V as the B-field is lowered, as shown in Table 1. By contrast, the peak values in the discharge current I_d, decrease significantly (by ~ 65%) with lowering B-field, with average currents $\langle I_d \rangle$ decreasing from 183 to 128 A. Similar trends are seen at 75 and 150 Hz HiPIMS frequencies and also in pulsed DC conditions, but these are not shown. The observation that I_d decreases as the magnets are withdrawn is consistent with the idea that lower B-fields lead to a loss of electron confinement and lower plasma densities. To maintain a constant power V_d must necessarily rise over the pulse period as observed.

3. Results and discussions

3.1 The effect of magnetic field on deposition rates

The measured deposition rates for HiPIMS, DC and pulsed-DC sputtering over the range in B-field strengths are shown in figure 4. For conventional sputtering the rates are lower for reduced magnetic strengths due to a loss in plasma confinement. The deposition rate falls by about 25 to 40% between BF1 and BF4. The increased discharge voltages with lower B-fields cannot compensate, via higher sputter yields, for the fall in plasma density. This can be seen from examination of the DC data (in table 1). A 13% increase in the DC target voltage (from 260 to 296 V) as B is reduced would only lead to a similar increase in sputter yield over this small range in ion bombarding energies.

yiled Figure 4 also reveals lower deposition rates for higher pulsed-DC frequencies, which can be understood on the basis of the arguments proposed in [18] in that there is a dead-time (500 to 1000 ns) associated with each pulse ‘on-time’. This is the formative time lag described by Anders [19]. During this dead-time, negligible amounts of sputtering take place. This dead-time becomes an increasingly significant proportion of the pulse on-time as the pulse frequency is increased. In contrast, for HiPIMS, the magnetic field strengths influence the deposition rate in the opposite sense showing a marked increase in the deposition rates with weaker fields (see the dotted curves in figure 4). For example at a frequency of 100 Hz the deposition rate nearly doubles (from 7.5 to 14.7 nm min^{-1}) as we go from BF1 to BF4.

These observations agree well with those of Capek et al [16] in which the deposition rate of Nb increased by a factor of ~4.5 (from 10.6 to 45.2 nm min^{-1}) through a 30% reduction in the parallel component of the B-fields at the target (from 1031 to 716 G). Our results also agree in trend with results from the sputtering of Cr in which an increase of 70% in the power normalized deposition rate (from 270 to 360 nm h^{-1} kW^{-1}) was measured for a decrease in the transverse magnetic field of 33% (from 50 mT to 17 mT) [20].

Although significantly lower discharge currents are recorded with weaker B fields (figure 2) due to the fall in plasma density, in the case of HiPIMS this actually leads to an increase in deposition rate. In agreement with pulsed-DC sputtering, HiPIMS deposition rates decrease with pulse frequency and the argument of dead-time [18] may apply here.

One crucial difference between HiPIMS and conventional magnetron sputtering is the high degree of ionisation of the metal sputtered flux and that the dominant deposition species in HiPIMS are ions (e.g. in our case Ti^{+} and possibly multi-charged ions) rather than neutrals. Based on ideas developed by Mishra et al [12] we argue that these ions are affected by the positive-going potential structure (seen in all magnetron systems) ahead of them in the bulk plasma and can be reflected back to the cathode if their kinetic energy is less than the equivalent of the hill potential. The potential barrier (of the order of 10’s of volts) increases in height with increasing B-fields

strengths [12] effectively filtering out ions, allowing only post-ionized sputtered atoms in the tail of the Sigmund-Thomson sputtering distribution (see [2]) to reach the substrate. Clearly, this affect will be important in HiPIMS discharges but not in conventional sputtering configurations with deposition dominated by neutrals.

In HiPIMS it appears that as we weaken the magnetic field and reduce the electron confinement efficiency, the potential hill (pre-sheath structure) self-consistently decreases in height allowing proportionally more metallic ions to the substrate. Although less metallic ions are created in the plasma with weaker fields the loss in confinement of ions wins as a competing effect and the deposition rate (of a deposit formed from of these ions) increases.

3.2 Calculation of return probabilities based on a simple model

To be able to quantify better the expected deposition rates in HiPIMS plasmas Christie [17] developed a simple particle flux model incorporating back attraction and scattering loss of ionic components. This model was later modified and updated by Vlcek et al.,[21], Lundin [22] and Vlcek and Burcalova [23], providing a link between the probability of ionization (α) and back attraction to the target (β) of the sputtered vapour to the flux of species to the substrate. The more sophisticated model of Vlcek and Burcalova [23] with the inclusion of secondary electron release and collisional energy loss provides a prediction for the product of the metal ionization and return probabilities αβ that scale with the target voltage as $V_d^{-1/2}$.

Here we develop a simple 0-D particle flux model (similar to that of Christie [17]) which can be used in conjunction with our experimental data from the different sputtering modes to predict HiPIMS behaviour in terms of back attraction with changing magnetic field. In the model, the probability of a sputtered metal atom being ionised in the plasma we assign as α with β being the probability it will return to the cathode. For simplicity, we will ignore other processes that can lead to recapture of the metal species, such as collisional scattering and multiple reflection from surfaces. We assume that in DC sputtering there are few metallic ions and therefore they play an insignificant role in the deposition process, however in HiPIMS they have a dominating role and the number of metal ions reaching the substrate will be governed by the term α(1- β), a measure of the effective loss of confinement of ionized metals.

Let us consider the processes at the titanium target, irrespective of the sputtering mode, assuming no contribution from multiply charged metal ions. The instantaneous flux of sputtered neutral metal atoms leaving the target can be written as

$$\Gamma_{Ti}^{N} = \gamma_{Ar}\Gamma_{Ar}^{+} + \gamma_{Ti}\Gamma_{Ti}^{+} \qquad (1)$$

where Γ_{Ar}^{+} and Γ_{Ti}^{+} are the argon and titanium ion fluxes to the target and γ_{Ar} and γ_{Ti} are the respective sputter yields. If the probability of ionisation of neutral metal is α and the probability of return of the metal ion to the cathode is β, the total flux Γ_{Dep} of titanium (both ion and atom) at the substrate assuming no other losses *en route* would be,

$$\Gamma_{\mathrm{Dep}} = \alpha(1-\beta)\Gamma_{Ti}^{N} + (1-\alpha)\Gamma_{Ti}^{N} \qquad (2)$$

However, if we consider the possibility of geometric and collisional losses between target and substrate for both ionic and neutral species then we could modify (2) to

$$\Gamma_{\mathrm{Dep}} = G_{Ti^{+}}\alpha(1-\beta)\Gamma_{Ti}^{N} + G_{Ti^{0}}(1-\alpha)\Gamma_{Ti}^{N} \qquad (3)$$

where $G_{Ti^{+}}$and $G_{Ti^{0}}$ represent the effective loss of ionic and neutral titanium species, terms however not to be determined in the model.

The flux of titanium ions returning to the cathode is

$$\Gamma_{Ti}^{+} = \alpha\beta\Gamma_{Ti}^{N} \qquad (4)$$

Assuming similar geometric and scattering loss for metal ions and neutrals then the unknown factors can be written $G_{Ti^{+}} \sim G_{Ti^{0}} = \mathrm{G}$ (<1) so that equation 3 above is simplified to

$$\Gamma_{\mathrm{Dep}} = (1-\alpha\beta)G\Gamma_{Ti}^{N} \qquad (5)$$

The total effective positive ion flux at the cathode Γ_{d} carrying the discharge current $I_d (= eA\Gamma_{\mathrm{d}})$ to the race track of area A is given by

$$\Gamma_{\mathrm{d}} = (1 + \delta_{Ar})\Gamma_{Ar}^{+} + (1 + \delta_{Ti})\Gamma_{Ti}^{+} \qquad (6)$$

where δ_{Ar} and δ_{Ti} are secondary electron coefficients for argon and titanium ion bombardment of the cathode respectively. Here we will assume δ_{Ti}~0 as discussed in [19].

Combining equations 1, 3, 4, 5 and 6 we obtain an effective deposition flux from all metal species at the substrate namely,

$$\Gamma_{\mathrm{Dep}} = \frac{G(1-\alpha\beta)\gamma_{Ar}\Gamma_{\mathrm{d}}}{(1+\delta_{Ar})+\alpha\beta(\gamma_{Ar}+\gamma_{Ti}(1+\delta_{Ar}))} \qquad (7)$$

From this general case we can assign deposition fluxes for HiPIMS and DC sputtering as Γ_{Dep}^{HiPIMS} and Γ_{Dep}^{dc} respectively. For DC sputtering at cathode voltage V_{dc} we assume αβ ~0, and Γ_{Dep}^{dc} is written

$$\Gamma_{Dep}^{dc} = \frac{G_{dc}\gamma_{Ar}(\mathrm{V}_{dc})\Gamma_{\mathrm{d}}(\mathrm{V}_{dc})}{1+\delta_{Ar}(\mathrm{V}_{dc})} \qquad (8)$$

and correspondingly for HiPIMS

$$\Gamma_{Dep}^{HiPIMS}(t) = \frac{G_{HiPIMS}(1-\alpha\beta)\gamma_{Ar}(t)\Gamma_{\mathrm{d}}(t)}{(1+\delta_{Ar}(t))+\alpha\beta(\gamma_{Ar}(t)+\gamma_{Ti}(t)(1+\delta_{Ar(t)}))} \qquad (9)$$

where time-varying parameters have been introduced for HiPIMS, and the loss parameters G are now specific to the particular mode of sputtering. However, experimentally we do not measure instantaneous deposition fluxes but time-averaged deposition rates. These we will assign as D_{HiPIMS} and D_{dc} for the HiPIMS and DC sputtering cases respectively. Since DC and HiPIMS plasmas were struck in the same system and at the same operating pressure we assume the geometrical and scattering processes represented by the terms G in equations 8 and 9 are similar between the different modes (i.e. $G_{\mathrm{HiPIMS}} \sim G_{dc}$). Eliminating these terms from the above equations

and acknowledging that we must integrate over the entire pulse period T to convert fluxes (Γ_{Dep}^{HiPIMS}, Γ_{Dep}^{dc}) to deposition rates (D_{Hipims} , D_{dc}) we get

$$1 = \frac{D_{HiPIMS}}{D_{dc}} \frac{(1+\delta_{Ar}(V_{dc}))}{\gamma_{Ar}(V_{dc}) I_{dc} T} \int_0^T \frac{(1-\alpha\beta)\gamma_{Ar}(t) I_d(t)}{(1+\delta_{Ar}(t))+\alpha\beta(\gamma_{Ar}(t)-\gamma_{Ti}(t)(1+\delta_{Ar}(t)))} dt \qquad (10)$$

where targets fluxes $\Gamma_d(t)$ and $\Gamma_d(V_{dc})$ have been converted to measured currents $I_d(t)$ and I_{dc} respectively. The secondary electron coefficient δ_{Ar} at low energies is governed by *potential emission* [19], and insensitive to ion energy and we assign here a constant, but realistic, value of 0.06, taking into account a recapture probability for emitted electron at the target of 0.5 [2].

Using equation (10) with quantities, D_{HiPIMS}, D_{dc}, $I_d(t)$, I_{dc}, $V_d(t)$, V_{dc} and T, all taken from experiment, the compound probability of ionisation and target return αβ can be calculated. This is shown in figure 5 and tabulated in table 1 as a function of the four different magnetic field cases, BF1 – BF4. Here the sputter yields γ_{Ar} and γ_{Ti} were approximated by functions of ion energy (the target voltages V_d (t)) with data taken from an on-line calculator [24], based on empirical equations for sputter yields at normal incidence [25]. The data was fitted to a convenient functional form $\gamma \sim a(V_d - V_{d0})^n$ where V_{d0} is the sputtering threshold and *a* and n are fitting parameters.

Figure 5 shows clearly, at all HiPIMS frequencies, a fall in αβ with decreasing magnetic field strength, corresponding to higher ionic fluxes and higher deposition rates at the substrate $\propto$ (1- αβ). The most marked decrease is seen at 75Hz where αβ falls from 0.9 to 0.7, a 22% drop corresponding to a 110% increase in deposition rate. Clearly, HiPIMS deposition rates are highly sensitive to the compound probability of metal neutral ionisation and target return.

The calculated tends in αβ agree well with those found by Capek et al [16], who used a more sophisticated model incorporating terms for transport loss of ions. From measured target mass loss rates they calculate a fall in αβ from 0.71 to 0.46 with decreasing B-field (30% reduction), while deposition rate measurements showed αβ to decrease from 0.83 to 0.36 over the same range in B-field strengths. Although these changes in αβ are somewhat larger our predictions (0.9 to 0.7), possibly due to

differences in the complexity of the respective models, the different target materials and plasma condition, our results for Ti do support the conclusions by Capek et al [16], that the return effect (represented by αβ) is the most important phenomena lowering deposition rates in HiPIMS.

Figure 6 shows the correlation between αβ and the average discharge voltage $<V_d>$. The $<V_d>$ values are shown in table 1. It reveals a quasi-linear falling relationship, insensitive to the pulse frequency. The basic trend that αβ falls with increasing V_d agrees with Vlcek and Burcalova [23] however here somewhat more quickly than their predicted rate of $\alpha\beta \propto V_d^{-1/2}$. Here, we have not considered electron energy balance in the flux formulation, only particles continuity together with measured deposition rates, unlike the analysis in [23] in which expressions for α and β have been generated more explicitly.

The results demonstrate that as the B-field is lowered there is a reduction in the ion return probability together with relaxation in the effective plasma confinement in the plasma bulk. We understand this from the stand point of manipulation of the positive going potential hill (extended pre-sheath) that exists in the axial direction from target to substrate through variation of the magnetic field strength of the trap. Strong axial electric fields exist to drive electron transport across the magnetic fields to preserve current continuity. Diminishing B-fields self-consistently lead to lower bulk potential drops as observed in [12], allowing a larger fraction of sputtered metal particles created close to the target to reach the substrate. This accounts for the lower predicted values of αβ and concomitant increases in deposition rate as we go from configuration BF1 to BF4.

So counter intuitively, in HiPIMS sputtering poorer plasma confinement with lower plasma densities and lower discharge currents actually give rise to increased deposition rates. However, one must note that progressively lowering the magnetic field strength will lead to a situation where the electron gyro radii eventually exceed the size of the magnetic trap and a total loss of the “magnetron effect”.

However, it is also important to consider the effect of changing the magnetic field on the thin fim structure and morphology. As described by Alami et al [26] in reactive HiPIMS of CrN films, stronger magnetic fields result in a decrease in the Cr_2N content indicating higher dissociation probabilities of N_2 (through stronger electron confinement) and the presence of smaller coating-forming crystals. The authors argue that therefore in HiPIMS the magnetic field strength and shape should be designed to give the optimum deposition rates and film structure.

4. Conclusions

A comparative study of titanium deposition rates in a magnetron system has shown markedly different behaviour between HiPIMS and conventional sputtering as the magnetic field strength is changed. In HiPIMS as the confining B-field is lowered the target currents reduce but the deposition rates actually increase significantly. At our chosen operating conditions (680W, 0.54Pa) they increase by a factor 2 when the magnetic field strength at the target is reduced by 45%. However, in DC and pulsed-DC modes we observe the expected behaviour that deposition rates fall (here by 25-40%),

Unlike conventional sputtering, in HiPIMS the deposition flux is dominated by metal ions. These particles must overcome the positive-going space potential that exists between the sheath edge and substrate to contribute to the deposition rate. We argue that lower B-fields lead to a relaxation of the requirement for strong axial electric fields to exist to drive cross-field electron transport, so allowing more ions (post-ionized neutrals with a sputter energy distribution) to reach the substrate.

Using a simple model of particle fluxes and measured deposition rates, we show that the compound probability of ion creation and return to the target drops from 0.9 to about 0.7 as the B-field strength is reduced The results show a near linear decrease in this probability with increasing average discharge voltage. This study shows that magnetic field strength is a crucial parameter in determining HiPIMS deposition rates. We suggest that for users of HiPIMS the magnetron sources themselves should be properly designed in terms of magnetic geometry and strength to maximize deposition rates.

Acknowledgments

We wish to thank Mr TJ Petty for his efforts in replotting the figures as well as the EPSRC for their funding support.

References

[1] U Helmersson, M Lattemann, J Bohlmark, AP Ehiasarian, JT Gudmundsson Thin Solid Films 513, (2006), 1

[2] JT Gudmundsson, N Brenning, D Lundin and U Helmersson, J. Vac. Sci. Technol. A 30 (3), (2012), 030801

[3] A Anders, J. Vac. Sci. Technol. A 28, (2010), 783

[4] RK Waits, J. Vac Sci. Technol. 15, (1978), 179

[5] AE Ross, R Sangines, B Treverrow, MMM Bilek, and DR McKenzie, Plasma Sources Sci. Technol. 20, (2011), 035021

[6] M Samuelsson, D Lundin, J Jensen, MA Raadu, JT Gudmundsson, and U Helmersson, Surf. Coat. Technol. 202, (2010), 591

[7] S Konstantinidis, JP. Dauchot, M Ganciu, and M Hecq, J. Appl. Phys. 99, (2006), 013307

[8] K Macak, V Kouznetsov, J Schneider, U Helmersson and I Petrov, J. Vac. Sci. Technol. A 18, (2000), 1533

[9] D Horwat and A Anders, J. Phys. D: Appl. Phys. 41, (2008),135210

[10] D Lundin, P Larsson, E Wallin, M Lattemann, N Brenning, and U Helmersson, Plasma Sources Sci. Technol. 17, (2008), 035021

[11] T de los Arcos, R Schroder, Y Aranda Gonzalvo, V Schulz-von der Gathen and J Winter, Plasma Sources Sci. Technol. 23, (2014), 054008

[12] A Mishra, PJ Kelly, and JW Bradley, Plasma Sources Sci. Technol.19, (2010) 045014

[13] S Konstantinidis, JP Dauchot, M Ganciu, and M Hecq, Appl. Phys. Lett. 88, (2006) 021501

[14] J Vlcek, B Zustin, J Rezek, K Brucalova, and J Tesar, Society of Vacuum Coaters 52nd Annual Technical Conference Proceedings, Santa Clara, CA, 9–14 May 2009 (Society of Vacuum Coaters, Albuquerque, NM), pp. 219–223

[15] PM Barker, E Lewin and J Patscheider, J. Vac. Sci. Technol. A 31 (2013) 060604

[16] J Capek, M Hala, O Zabeida, O. JE Klemberg-Sapieha and L Martinu, J Phys. D: Appl. Phys. 46 (20), (2013), 205205

[17] DJ Christie, J. Vac. Sci. Technol. A 23, (2005), 330

[18] PJ Kelly, AA Onifade, Y Zhou, GCB Clarke, M Audronis and JW Bradley, Plasma Process Polym., 4, (2007), 246

[19] A Anders, Surf. Coat. Technol. 205, (2011), S1

[20] AP Ehiasarian and A Vetushka, Proceedings of 52nd SVC Technical Conference 2009, Santa Clara, 9-14 May (2009) page 265

[21 J Vlcek, P Kudlacek, K Burcalova and J. Musil, J. Vac. Sci. Technol. A 25, (2007), 42

[22 D Lundin, “The HiPIMS process,” Ph.D. thesis (Linkoping University, Sweden, (2010), Linkoping Studies in Science and Technology, Dissertation No. 1305

[23] J Vlcek and K Burcalova, Plasma Sources Sci. Technol. 19, (2010), 065010

[24] http://www.iap.tuwien.ac.at/www/surface/sputteryield

[25] N Matsunami, Y Yamamura, Y Itikawa, N Itoh, Y Kazumata, S Miyagawa, K Morita, R Shimizu, and H Tawara, in Energy Dependence of the Yields of Ion-Induced Sputtering of Monatomic Solids, IPPJ-AM-32 (Institute of Plasma Physics, Nagoya University, Japan, 1983)

[26] J Alami, Z Maric, H Busch, F Klein, U Grabowy and M Kopnarski, Surf. Coat. Technol. 255 (2014) 43

Figure Captions

Figure 1. A schematic diagram of the magnetron configuration including the B-field lines and the deposition rate monitor position, lying on a line above the racetrack.

Figure 2. The variation of total measured magnetic field strength $|B| = \sqrt{B_z^2 + B_r^2}$ on a line between the racetrack and the deposition rate monitor as the two sets of permanent magnets (poles) behind the target are withdrawn to larger distances (BF1 to BF4).

Figure 3. The HiPIMS cathode voltage V_d and current I_d waveforms for an average discharge power of 680 W and a gas pressure of 0.54 Pa at the four different magnetic field configurations, BF1 to BF4.

Figure 4. A plot of deposition rates versus decreasing magnetic field strengths, BF1 to BF4 for HiPIMS, DC and pulsed-DC modes of operation.

Figure 5. The predicted values of the product of the probabilities for metal ionization and return to the target (αβ) for decreasing magnetic field strengths, BF1 to BF4.

Figure 6. The modelled values of αβ vesus average discharge voltage V_d during the HiPIMS pulse for decreasing magnetic field strengths, BF1 to BF4.

Table captions

Table 1. The important parameters used in the model with predations for αβ.

Figures

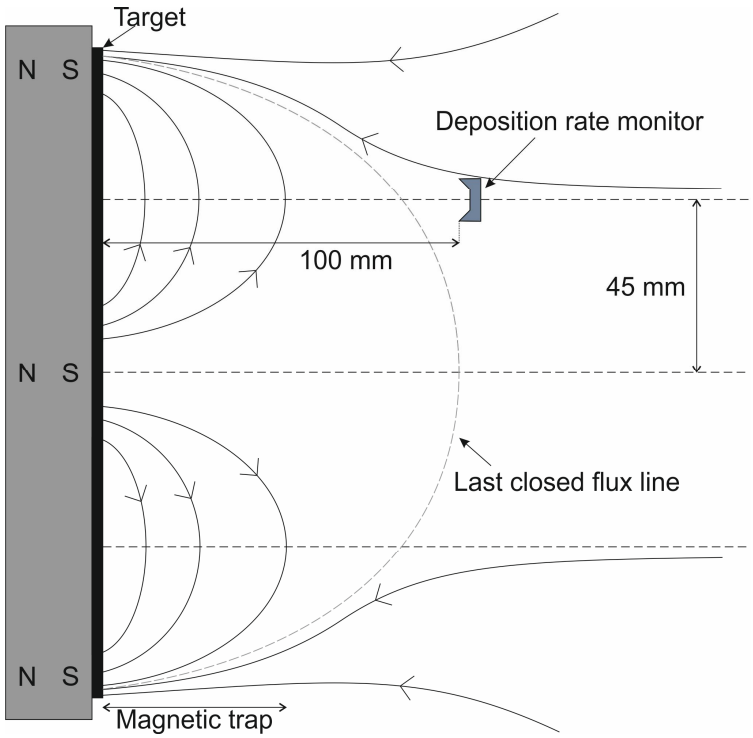

Figure 1

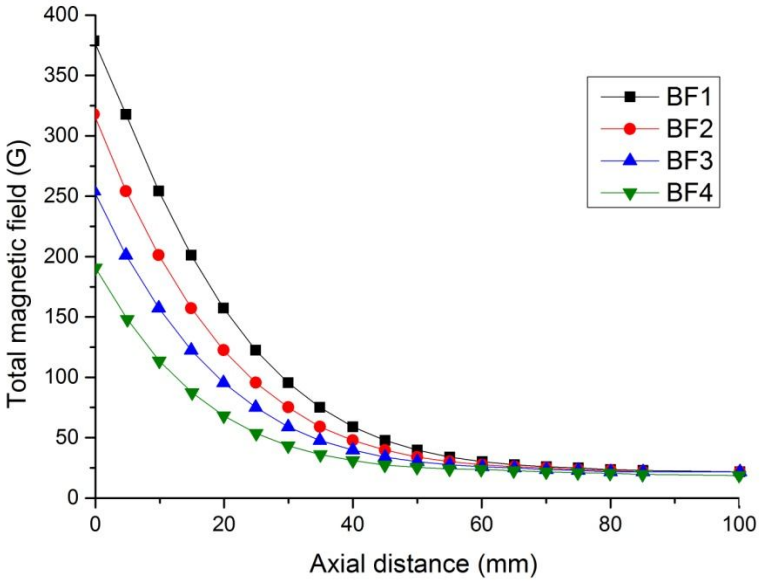

Figure 2

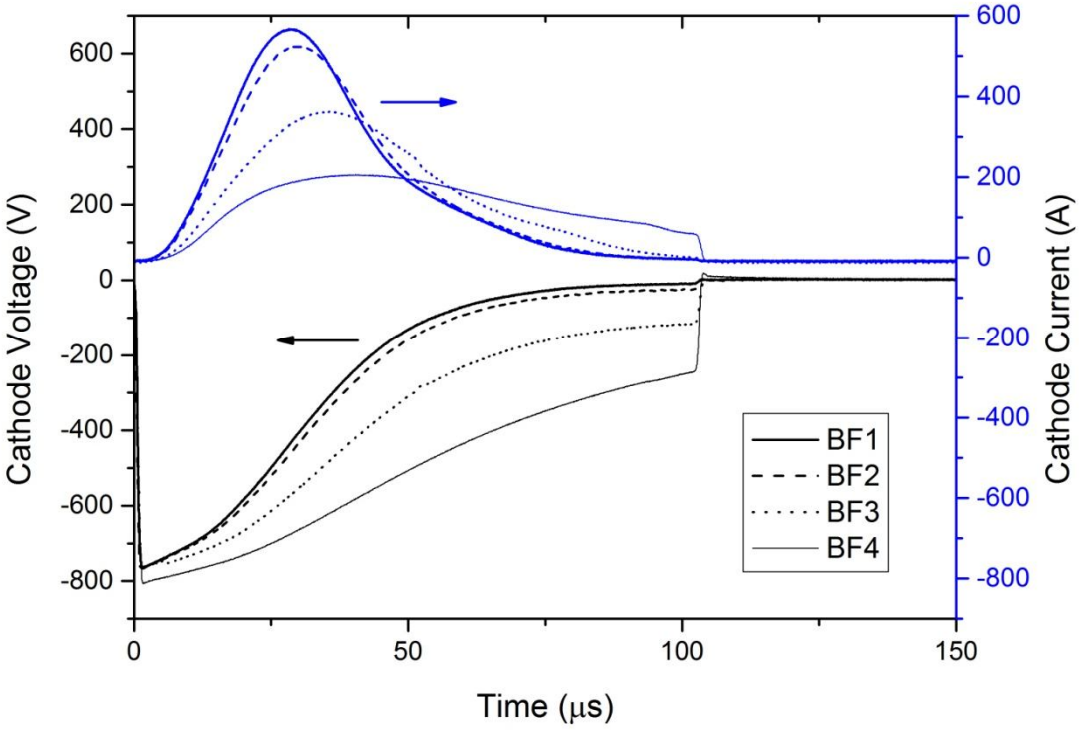

Figure 3

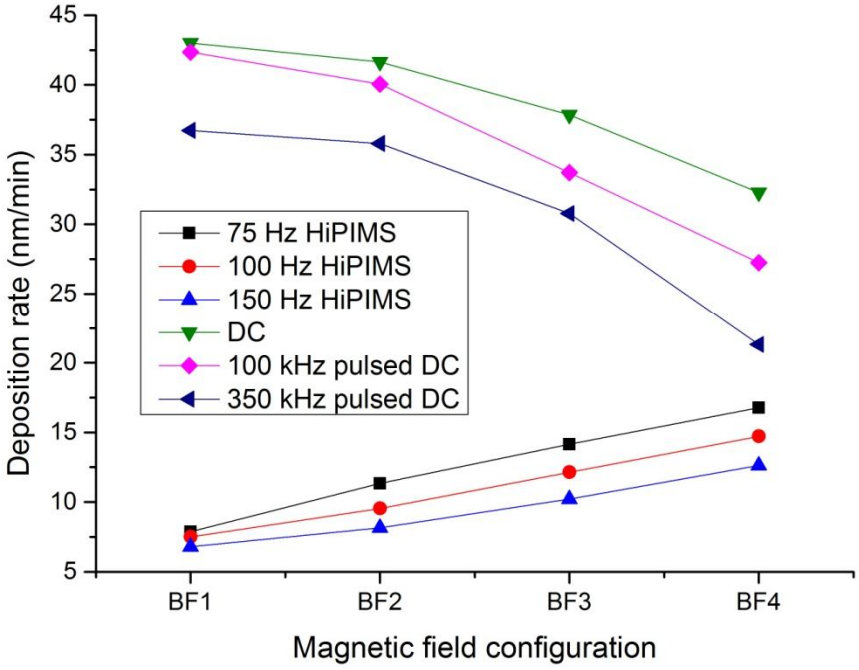

Figure 4

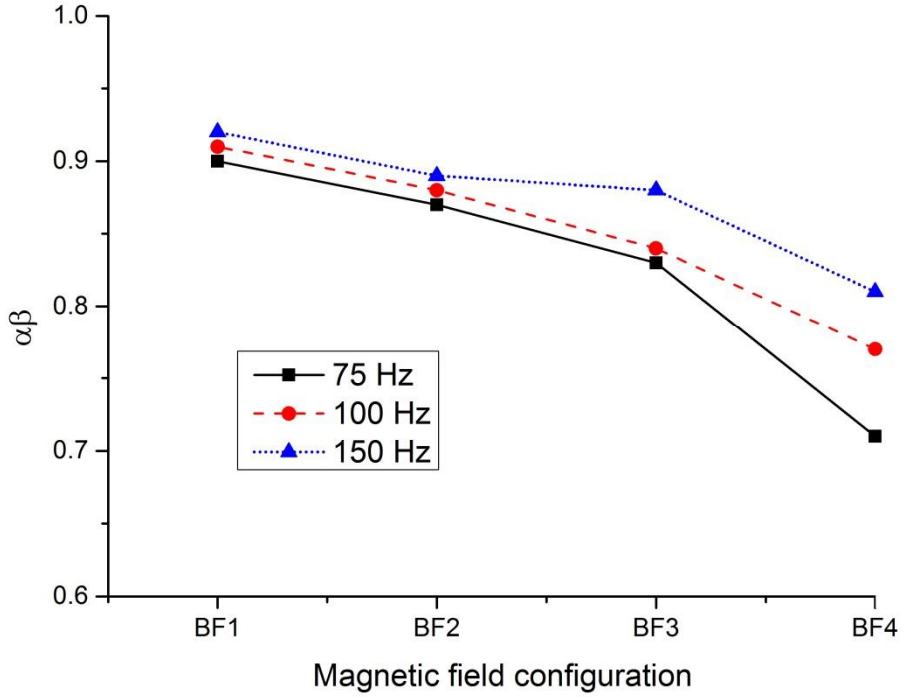

Figure 5

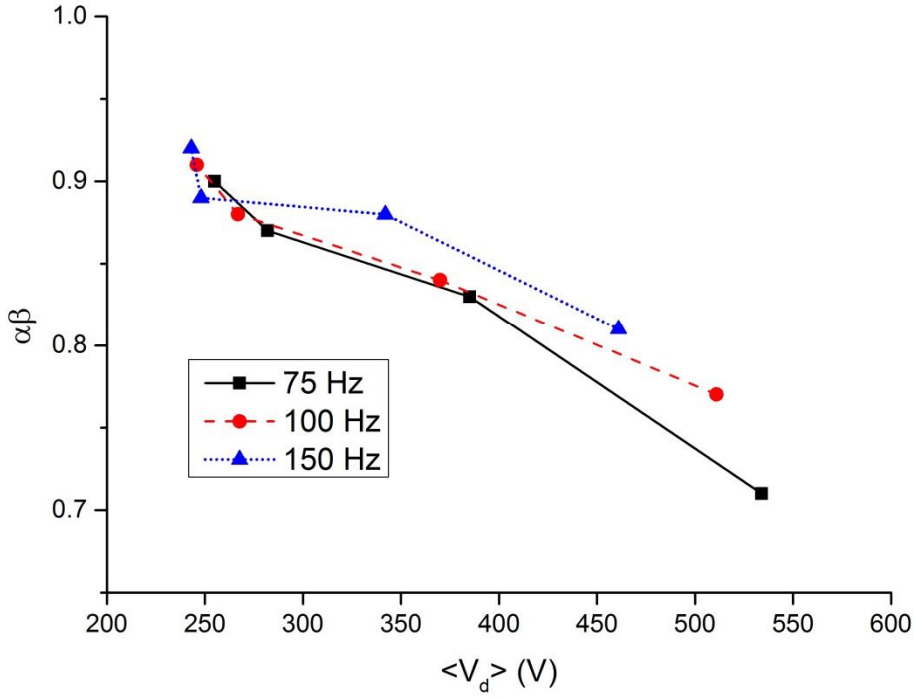

Figure 6

Table 1

B-field conf.	B at the target surface (G)	$<V_d>$ 75Hz	$<V_d>$ 100Hz	$<V_d>$ 150Hz	$<V_d>$ DC	Dep. rate 75Hz-nm/min	Dep. rate 100Hz nm/min	Dep. rate 150Hz nm/min	Dep. rate DC nm/min	$\alpha\beta$ 75Hz	$\alpha\beta$ 100Hz	$\alpha\beta$ 150Hz
BF1	355	255	246	243	260	7.87	7.50	6.80	43.00	0.90	0.91	0.92
BF2	340	282	267	248	272	11.35	9.54	8.16	41.64	0.87	0.88	0.89
BF3	255	385	370	342	285	14.15	12.14	10.22	37.86	0.83	0.84	0.88
BF4	190	534	511	461	296	16.77	14.72	12.63	32.28	0.71	0.77	0.81